THE JOURNAL OF BIOLOGICAL CHEMISTRY
Vol. 275, No. 37, Issue of September 15, pp. 28873–28881, 2000

Printed in U.S.A.

Identification and Functional Characterization of Human Soluble Epoxide Hydrolase Genetic Polymorphisms*

Received for publication, February 1, 2000, and in revised form, May 25, 2000
Published, JBC Papers in Press, June 20, 2000, DOI 10.1074/jbc.M001153200

Martin Sandberg‡, Christopher Hassett§, Elinor T. Adman¶, Johan Meijer‡, and Curtis J. Omiecinski§‖

From the ‡Department of Plant Biology, Uppsala Genetic Center, Swedish University of Agricultural Sciences, SE-750 07 Uppsala, Sweden, the §Department of Environmental Health and ¶Department of Biological Structure, University of Washington, Seattle, Washington 98105-6099

Human soluble epoxide hydrolase (sEH), an enzyme directing the functional disposition of a variety of endogenous and xenobiotic-derived chemical epoxides, was characterized at the genomic level for interindividual variation capable of impacting function. RNA was isolated from 25 human liver samples and used to generate full-length copies of soluble epoxide hydrolase cDNA. The resulting cDNAs were polymerase chain reaction amplified, sequenced, and eight variant loci were identified. The coding region contained five silent single nucleotide polymorphisms (SNPs) and two variant loci resulting in altered protein sequence. An amino acid substitution was identified at residue 287 in exon 8, where the more common arginine was replaced by glutamine. A second variant locus was identified in exon 13 where an arginine residue was inserted following serine 402 resulting in the sequence, arginine 403–404, instead of the more common, arginine 403. This amino acid insertion was confirmed by analyzing genomic DNA from individuals harboring the polymorphic allele. Slot blot hybridization analyses of the liver samples indicated that sEH mRNA steady-state expression varied approximately 10-fold. Transient transfection experiments with CHO and COS-7 cells were used to demonstrate that the two new alleles possess catalytic activity using *trans*-stilbene oxide as a model substrate. Although the activity of the glutamine 287 variant was similar to the sEH wild type allele, proteins containing the arginine insertion exhibited strikingly lower activity. Allelic forms of human sEH, with markedly different enzymatic profiles, may have important physiological implications with respect to the disposition of epoxides formed from the oxidation of fatty acids, such as arachidonic acid-derived intermediates, as well in the regulation of toxicity due to xenobiotic epoxide exposures.

Epoxides, three-membered strained organic configurations of oxygen, are formed enzymatically in cells and tissues during the oxidative metabolism of both endogenous and xenobiotic substances. Epoxide intermediates are often chemically reactive and unstable in aqueous environments. Consequently, a number of chemical epoxides have been implicated as critical initiators of diverse cellular damage, including protein and RNA adduction as well as genetic mutation (1, 2). Cellular regulation of epoxide disposition is therefore a decisive issue underlying mechanisms of molecular toxicology.

Five structurally distinct epoxide hydrolases (EC 3.3.2.3) have been identified in vertebrates, and these can be distinguished based on their respective physical properties of molecular weight, pH optima, and cellular localization (2). DNA encoding mammalian soluble epoxide hydrolase (sEH[1]; formerly referred to as cytosolic EH) has been characterized from human (3), mouse (4), and rat (5), as well as bacterial (6, 7) and plant species (8, 9). The human sEH gene *EPHX2*, is localized to chromosome 8p21-p12 (10), whereas the xenobiotic-metabolizing microsomal EH (mEH) gene, *EPHX1*, has been placed at 1q42.1 (11). Other epoxide hydrolases that have been identified include a cholesterol-metabolizing microsomal enzyme (12), and two soluble proteins, hepoxilin hydrolase (13) and leukotriene A_4 hydrolase (14). These three epoxide hydrolases have very limited and unique substrate specificities and, at least in the latter instance, a different catalytic mechanism.

Endogenous epoxides may be important effector molecules eliciting hormone-like responses in various organ systems. For example, arachidonic acid undergoes oxidization to an array of monoepoxides that can be enzymatically hydrolyzed to corresponding dihydrodiols (15–17). These metabolites can possess vasodilatory properties on the vascular system, with specific arachidonic acid epoxides and corresponding diol regioisomers exhibiting different physiological potencies (18). Recently, arachidonic acid 11,12-epoxide was demonstrated to function as an endothelium-derived hyperpolarizing factor, following generation via a cytochrome P450 2C-mediated reaction (19). In endothelial cells, cytochrome P450 2J2 has been identified as a potential source of epoxyeicosatrienoic acids that function to inhibit leukocyte adhesion to the vascular wall (20). Regulation of epoxyeicosatrienoic acid incorporation into phospholipids, a mechanism to modulate their biological effects, is likely mediated by sEH (21). Thus, regulation of the respective epoxygenase activities, in concert with the hydrolytic reactions catalyzed by epoxide hydrolase, are likely to be important de-

* This work was supported in part by the Swedish University of Agricultural Sciences, Swedish Medical Research Council Grant K99-72X-12225-03A, Magnus Bergvalls Stiftelse, Clas Groschinskys Minnesfond, Foundation for Strategic Research and Perssons Fund, and NIEHS National Institutes of Health Grants ES04978 and P30 ES07033. The costs of publication of this article were defrayed in part by the payment of page charges. This article must therefore be hereby marked "*advertisement*" in accordance with 18 U.S.C. Section 1734 solely to indicate this fact.

The nucleotide sequences for the soluble epoxide hydrolase clones reported in this study have been submitted to the GenBank™/EMBL Data Base with accession numbers AF233334, AF233335, and AF233336.

‖ Burroughs Wellcome Fund Toxicology Scholar. To whom correspondence should be addressed: Dept. of Environmental Health, University of Washington, 4225 Roosevelt Way NE, Seattle, WA 98105-6099. Tel.: 206-543-1700; Fax: 206-685-4696; E-mail: cjo@u.washington.edu.

[1] The abbreviations used are: sEH, soluble epoxide hydrolase; CAT, chloramphenicol acetyltransferase; CHO, chinese hamster ovary; mEH, microsomal epoxide hydrolase; *t*-SO, *trans*-stilbene oxide; Wt, wild type.

terminants of blood pressure control and inflammatory processes.

Another important lipid epoxide is the linoleic acid-derived product leukotoxin (*cis*-9,10-epoxyoctadec-12(*Z*)-enoic acid), which is associated with multiple organ failure and adult respiratory distress syndrome seen in some severe burn patients (22). Recently, evidence was presented indicating that the leukotoxin diol metabolite, generated by sEH, is a likely initiator of this severe toxicity (23). Soluble epoxide hydrolase may thus support both advantageous and deleterious reactions in its role as a processor of endogenous epoxides.

Mammalian sEH proteins demonstrate amino acid conservation in excess of 70%, as deduced from full-length cDNA clones (24). In particular, the carboxyl-terminal region of the primary sequences are very highly conserved among these mammalian species, approaching 87% similarity (including conservative amino acid substitutions). Little is currently known with respect to interindividual human sEH protein sequence variation. Comparison of the deduced amino acid sequences derived from two reports (3, 25) shows inconsistencies at 3 positions and predicts human sEH proteins of differing length (554 *versus* 555 residues).

Interindividual human sEH variation has been implied from studies showing differences in specific activity (26), in the metabolism of epoxide-containing drugs (27) and in correlative aspects of sister-chromatid exchange in leukocytes (28). In addition, individuals with high blood levels of fatty acid epoxides and cholesterol epoxides have been identified (29, 30). These phenotypes may be due simply to differences in relative enzyme levels (*e.g.* due to differences in sEH penetrance), or to the presence of allelic differences. Genetic polymorphisms influencing sEH structure may be envisioned that alter epoxide hydrolysis efficiencies, thus impacting important physiological processes requiring a distinct balance between cellular levels of epoxides and their corresponding dihydrodiols.

In the present investigation, we identify and characterize allelic variation in the transcribed region of the human soluble epoxide hydrolase gene. The nucleotide sequence polymorphisms discovered include nonconservative alterations that encode changes at two amino acid loci. *In vitro* expression and transient transfection experiments demonstrate that the sEH allelic variants are catalytically active, but exhibit distinctive biological behavior.

EXPERIMENTAL PROCEDURES

Materials—Oligonucleotides were obtained from Amersham Pharmacia Biotech or Life Technologies, Inc. (Täby, Sweden). Restriction enzymes and DNA modifying enzymes were from Roche Molecular Biochemicals (Mannheim, Germany) or Life Technologies, Inc., if not stated otherwise. Radiochemicals were from Amersham Pharmacia Biotech (Bucks, United Kingdom). DNA sequence analyses were performed on an ABI Prism 310 Genetic Analyzer, or an ABI Prism 377 DNA Sequencer, using the ABI Prism BigDye or dRhodamine Terminator Cycle Sequencing chemistry (Perkin-Elmer, Chatsworth, CA).

Human Liver RNA—Total RNA isolated from the livers of 25 unrelated individuals in an organ bank (31) was used to estimate steady-state expression, and for the synthesis of cDNA templates. Ten micrograms of total RNA from each of the liver samples was applied to a nylon membrane as described previously (31). [^{32}P]dCTP-labeled hybridization probe, derived from the wild type sEH full-length cDNA, was random primed (Ambion, Austin, TX), hybridized, and washed under stringent conditions (32). The membrane was stripped of the cDNA probe, and rehybridized with an oligomer complementary to 18 S rRNA essentially as described (33). Autoradiographic signals obtained from each probing were quantified using densitometry, and steady-state sEH mRNA levels were normalized to 18 S rRNA signal intensities (31).

Complementary DNA Synthesis—Five μg of total liver RNA was treated at 37 °C for 30 min with 0.5 units of DNase I (Promega Corp., Madison, WI) in a final volume of 9.5 μl including 10.5 mM dithiothreitol and 20 units of RNasin (Promega). After heat inactivation for 10 min at 72 °C, 260 ng of oligo(dT)$_{12–18}$ primer and 1.5 μl of dimethyl sulfoxide were added and samples were transferred to 42 °C. A prewarmed reaction mixture was added to each sample (final volume 20 μl), the temperature was increased slowly (approximately 15 min) to 50 °C, and incubation proceeded for 1 h followed by a 15-min incubation at 55 °C. The added premixture contained 1.0 μmol of Tris-HCl (pH 8.3), 1.5 μmol of KCl, 60 nmol of $MgCl_2$, 10 nmol of each dNTP, 0.1 μmol of dithiothreitol, and 100 units of SuperScript™ II reverse transcriptase (Life Technologies, Inc.). At the completion of first strand synthesis, samples were heat inactivated for 15 min at 70 °C and then treated with 2 units of RNase H to remove RNA complementary to the cDNA prior to PCR.

Amplification of sEH cDNA Samples—PCR amplification of the sEH-coding region was accomplished using a forward primer (5′-GCATCTCCCAGGTTAGCT-3′) located 35–52 base pairs upstream of the translation start codon, and a reverse primer (5′-TCCATGCAAGATGTGTGTA-3′) located 82–100 base pairs downstream of the translation stop codon. Thus, in addition to the coding region of human sEH that comprises 1668 nucleotides including the stop codon, an additional 35 base pairs of upstream and 82 base pairs of downstream sequence were characterized.

The Expand™ High fidelity PCR system (Roche Molecular Biochemicals) was used as per the manufacturer's directions, with the following modifications. Samples were initially heated at 94 °C for 3 min, and then amplified by 30–35 cycles of denaturation (25 s at 94°), annealing (30 s at 50 °C), and extension (2 min and 20 s at 72 °C). Finally, cDNA ends were flushed at 72 °C for 10 min. PCR products were purified on Qiaquick™ purification columns (Qiagen) before agarose gel electrophoresis to estimate quantity and purity of samples.

DNA Sequencing and Analysis—The purified PCR products were sequenced using a minimum of five primers targeted to the sEH cDNA. Additional primers also were employed in order to generate DNA sequence from the opposite strand for the resolution of discrepancies and to confirm the presence of polymorphic loci. New PCR reaction sets, and subsequent DNA sequencing, were similarly conducted to reconfirm polymorphisms and to exclude PCR artifacts where differences existed from the wild type (Wt) sequence. Data were initially collected and processed by Applied Biosystems DNA sequencing analysis software. Further assembly and editing of the files was performed using Genepro™ and MacVector™ computer software.

Cloning of sEH Alleles for in Vitro Expression—To determine the functional effects of amino acid variation, sEH alleles were obtained from individuals possessing polymorphisms and cloned into the pBluescript SK$^+$ vector. In this procedure, primers were modified to introduce unique *Bam*HI (forward primer: 5′-TA***GGATCC***CCCAGGTTAGCTGCG-3′) and *Xba*I (reverse primer: 5′-AT***TCTAGA***TGTGTGTAAGGCCACC-3′) restriction sites into the sEH PCR products (restriction sites are shown in bold italicized face; mismatches necessary to create artificial sites are underlined). The expected sequence of the constructs was confirmed by DNA sequencing of the resultant clones. Three unique sEH-allelic constructs were excised from the pBluescript hosts and subcloned into the *Bam*HI/*Xba*I sites of the eukaryotic expression vector pcDNA3 (Invitrogen, Carlsbad, CA). The sequence of each sEH allele was reconfirmed after subcloning. Plasmids were prepared using Wizard ion exchange columns from Promega. Quantitation and purity of the plasmids was determined by spectrophotometric readings and agarose gel electrophoresis.

Cell Culture and Transient Transfection—Both CHO and COS-7 cell lines were utilized for transient transfection experiments. Cells were grown at 37 °C in 95% air, 5% CO_2 (v/v) in Dulbecco's minimal essential medium (Life Technologies, Inc.) supplemented with 10% heat-inactivated fetal bovine serum (Sigma) and penicillin-streptomycin. Plasmid transfections were mediated by the Dosper™ liposomal reagent (Roche Molecular Biochemicals) according to the manufacturer's protocol. At the termination of each experiment, cells were washed three times in phosphate-buffered saline before harvest and centrifuged (400 × *g* for 5 min) at 4 °C followed by resuspension in ice-cold 0.25 M Tris-HCl (pH 7.5).

Time Course of sEH Expression—CHO or COS-7 cells were seeded in dishes with 5 ml of medium at a density of 4×10^5 cells/6-cm dish. The following day, at approximately 50% confluency, the media was replaced with 3 ml of serum-free medium and the cells were transfected with 2.025 μg of each human sEH allele or pcDNA3 construct, 0.225 μg of pcDNA3-CAT, and 9 μg of Dosper reagent. Six hours after transfection the medium was replaced with 5 ml of medium containing 10% fetal bovine serum. Cells were harvested for enzymatic analysis at several time points up to 48 h (CHO cells) or 58 h (COS-7 cells) following transfection.

sEH Protein Stability over Time—Petri dishes (10 cm diameter) were seeded with CHO or COS-7 cells in 13 ml of medium at a density of 2×10^6 cells per dish. The following day, when cells were approximately 50% confluent, the media was replaced with 6.5 ml of serum-free media and cells were transfected with 4.5 μg of each human sEH construct or pcDNA-3 vector, 0.4875 μg of pcDNA3-CAT and 19.5 μg of Dosper™ reagent. Six hours following transfection the media was replaced with 15 ml of media containing 10% fetal bovine serum. Cells were harvested 40 h after transfection, and stored at 4 °C until enzymatic assays were conducted over the course of 25 days. Each human sEH construct, or mock-transfected control, was performed in duplicate Petri dishes, and cells from each group were combined at the end of the experiment.

Enzymatic Activity of sEH Proteins—Preliminary experiments indicated certain sEH allelic proteins were especially sensitive to freeze-thaw procedures. Therefore, sEH enzyme measurements were subsequently performed on non-frozen cell extracts. Epoxide hydrolase activity was assayed (34) using *trans*-[^{3}H]stilbene oxide as substrate (*t*-SO). The final substrate concentration was 100 μM in 0.1 M potassium phosphate (pH 7.0). Incubations were performed at 37 °C for 1–2 h depending on the activity of the respective fractions. The substrate and product were separated by extraction with isooctane and an aliquot of the aqueous phase was analyzed by liquid scintillation spectroscopy. Potential background activity in the samples due to glutathione conjugation was taken into account by extracting the aqueous phase with hexanol. All measurements were performed at least in duplicate with fresh, resuspended non-lysed cells. Normalization of *t*-SO activity was achieved by the concurrent transfection of CAT-expressing plasmids with each sEH or mock-control transfection. The sEH wild type sample displaying the highest CAT expression at each time point was used to normalize the other samples according to their respective CAT activity. The variation in CAT activity was usually less than 15% between the samples.

CAT Assay—An aliquot of transfected CHO or COS-7 cells, resuspended in ice-cold 0.25 M Tris-HCl (pH 7.5), was lysed by 3 cycles of freeze-thawing, and centrifuged at 14,000 $\times$ *g* for 5 min at 4 °C. The supernatant was removed and briefly frozen in a dry ice/ethanol bath. Samples were subsequently stored at −20 °C until use. CAT assays were performed according to a protocol supplied with the expression plasmid pcDNA3 (Invitrogen). [^{14}C]Chloramphenicol and its acetylated products were separated by TLC on silica gel plates (LK6DF; Whatman Biosystems, Maidstone, UK). After overnight exposure to a PhosphorImager (Molecular Dynamics, Sunnyvale, CA), CAT activity was analyzed by densitometry using ImageQuant software (version 3.22; Molecular Dynamics).

Restriction Fragment Length Polymorphism/Southern Blot Analysis—Genomic DNA was isolated from four livers (numbers 127, 133, 135, and 137) and restricted with 4 enzymes (*Bam*HI, *Eco*RI, *Kpn*I, and *Sac*I). Ten micrograms from each digest were size-separated on a 0.85% agarose gel and transferred to a nylon membrane under denaturing conditions, as described previously (32). The Southern blotted DNA was hybridized with an sEH cDNA probe (prepared as described above), washed under stringent conditions (32), and exposed to x-ray film for 5 days.

RESULTS

Tissue Samples and Steady-state sEH mRNA Variation—The liver samples used in this study originated from a bank primarily composed of potential organ donors, and the demographic characteristics of this population have been described previously (33). Slot blot hybridization to random primed cDNA fragments confirmed that each of the 25 liver samples expressed sEH mRNA. Following normalization to 18 S rRNA levels, expression of sEH mRNA was determined to vary approximately 10-fold among individuals in this population as judged by quantitative computer densitometry of the resulting autoradiograms (data not shown).

sEH Sequence Variation—In the coding and flanking regions, 15 of 25 individuals possessed identical sEH nucleotide sequences, and this allele is designated wild type (Wt). The Wt sEH sequence was identical to that reported previously (25). However, the remaining 10 individuals demonstrated additional alleles, with polymorphisms located at eight distinct loci (Table I).

Only one individual was identified with a homozygous polymorphic locus, subject number 125, who possessed a silent transversion (C > A) at nucleotide 63 (Table I). It may be noteworthy that this sample was obtained from the only Hispanic individual in our study population, and the mutant locus was not observed in other samples. Other synonymous mutations within the sEH protein-coding region were observed at nucleotide positions 849, 921, 1236, and 1593. A base substitution was also detected in the 3′ noncoding region of the sEH transcript, at nucleotide 1703.

TABLE I
Nucleotide and corresponding amino acid sequences in the EPHX2 gene of 25 human subjects

The "A" residue of the initiator methionine codon (ATG) is denoted nucleotide +1. The numbering of nucleotides and amino acids is based on the published genomic *EPHX2* sequence (25). Wild type ("Wt") refers to the predominant allele, and is inferred unless stated otherwise. Polymorphism designations are according to recommendations (35).

Liver Sample	Nucleotide polymorphism	Amino acid polymorphism
104	^{1593}A > C, and ^{1703}A > G	
105	^{1593}A > C, and ^{1703}A > G	
106	Wt	
108	Wt	
109	^{1236}C > T, ^{1593}A > C, and ^{1703}A > G	
114	Wt	
118	^{860}G > A, ^{1593}A > C, and ^{1703}A > G	R287Q
119	Wt	
120	^{860}G > A, ^{1593}A > C, and ^{1703}A > G	R287Q
121	Wt	
124	Wt	
125	^{63}C > A; ^{63}C > A	
127	Wt	
128	Wt	
129	1206–1207insCGT	Arg$^{402–403ins}$
131	Wt	
133	^{849}G > A, ^{921}A > G, 1206–1207insCGT	Arg$^{402–403ins}$
134	Wt	
135	Wt	
136	Wt	
137	^{860}G > A, ^{1593}A > C, and ^{1703}A > G	R287Q
138	Wt	
139	Wt	
140	Wt	
141	^{860}G > A, ^{1593}A > C, and ^{1703}A > G	R287Q

The two remaining polymorphisms identified from these analyses were missense mutations, affecting sEH protein composition. Four individuals possessed a G > A substitution at nucleotide 860, located in exon 8. This change results in a nonconservative amino acid substitution of Gln for Arg at amino acid 287 of the sEH protein.

In addition, an insertion of the trinucleotide "CGT" after nucleotide 1206 in exon 13 was identified in two subjects (numbers 129 and 133). This mutation, which does not alter the reading frame, results in the insertion of an Arg residue immediately following Ser^{402}. This polymorphism was confirmed independently from genomic DNA isolated from samples 129 and 133 and amplified using a forward primer in intron 12 (5′-GGCACAGGTAGGGTGCTTG-3′) and a reverse primer in intron 13 (5′-CCCAGTAGAGTGAGGACCTC-3′) of the *EPHX2* gene. The resulting PCR products were sequenced and the trinucleotide insertion (encoding the additional Arg residue) was observed in both samples (in addition to the Wt allele), establishing that this polymorphism was not an artifact of reverse transcription during cDNA synthesis from sEH mRNA. The trinucleotide insertion is centrally located in exon 13 (25), thus a splice junction processing error is unlikely to explain its occurrence. As recommended (35), this insertion is designated Arg$^{402–403ins}$.

Human sEH polymorphisms identified in this investigation are summarized in Table II. A total of eight polymorphic loci were discovered in the 25 human sEH cDNA sequences (50

TABLE II
Human sEH polymorphisms identified in cDNA samples from 25 unrelated individuals

Nucleotide positions are referenced relative to human sEH sequence (25) not containing the Arg amino acid insertion designated as polymorphism 5, below. The "A" of the Met (ATG) initiator codon is denoted nucleotide +1.

Polymorphism[a]	Nucleotide position	Change	Frequency
			%
1	63	C > A	4
2	849	G > A	2
3	860	G > A	8
4	921	A > G	2
5	After 1206	CGT insertion	4
6	1236	C > T	2
7	1593	A > C	14
8	1703	A > G	14

[a] Polymorphism number 3 results in an Arg^{287}-Gln amino acid change. Polymorphism number 5 results in the insertion of an Arg residue after Ser^{402}.

alleles), including 5 transitions, 2 transversions, and 1 insertion. The observed frequency for each variant was greater than 1%, and therefore these represent true human genetic polymorphisms. Using the 5′-nuclease assay to discriminate alleles (36), we have now examined genomic DNA from more than 250 individuals for the presence of the 2 sEH amino acid polymorphisms. In this larger study, the Gln^{287} allele occurs at a frequency greater than 9%, while the $Arg^{402-403ins}$ mutation was found in approximately 7% of the alleles (data not shown).

Expression of Human sEH Alleles—The sEH alleles employed for transient protein expression studies were generated directly from cDNA samples in the study population. The R287Q allele was amplified from individual 118 and therefore also contains a silent $^{1593}A > C$ nucleotide substitution in the coding region; this particular allele contained the $^{1703}A > G$ transition in the 3′ noncoding portion of the transcript as well. The $Arg^{402-403ins}$ allele was amplified from individual 129 and is identical to the Wt nucleotide sequence, apart from the arginine insertion.

Time Course of sEH Expression—Nonlysed cell suspensions generated from each of the three sEH construct transfections (*i.e.* Wt, R287Q, and $Arg^{402-403ins}$) were used to determine sEH activity using *t*-SO as the substrate. Constructs of sEH alleles were transfected into both CHO and COS-7 cells which were harvested at multiple time points following transfection.

As shown in Fig. 1, *A* and *B*, each of the sEH allelic variants was catalytically active toward the *t*-SO substrate following transfection into CHO cells. Endogenous sEH activity, assessed from cells that were mock transfected with expression vector containing no insert, was at least 5-fold below the lowest expressing sEH allele. At each duplicate time point examined, the pattern of sEH enzymatic activity was highly consistent. CHO cells transfected with the Wt sEH allele demonstrated the highest enzyme activity, and the R287Q allele was more active than the $Arg^{402-403ins}$ variant.

At time points comparable to the CHO analysis, sEH alleles transfected into COS-7 cells (Fig. 2, *A* and *B*) produced similar enzymatic observations. The Wt allele was not as clearly distinguishable from the R287Q variant, but cells transfected with the $Arg^{402-403ins}$ allele consistently exhibited much lower sEH enzymatic activity. In these experiments, endogenous sEH activity was at least 3-fold lower than observed for the $Arg^{402-403ins}$ allele. A general trend of increasing sEH activity at later time points also distinguished COS-7 cell experiments from those conducted with CHO cells.

In preliminary experiments, the human sEH proteins have been overexpressed with His tags using *Pichia pastoris*, and purified proteins were isolated by nickel chromatography. Using *t*-SO as the substrate, the wild type and R287Q variant demonstrated equivalent enzymatic specific activity while the specific activity of the $Arg^{402-403ins}$ allele was reduced by approximately 40%.[2]

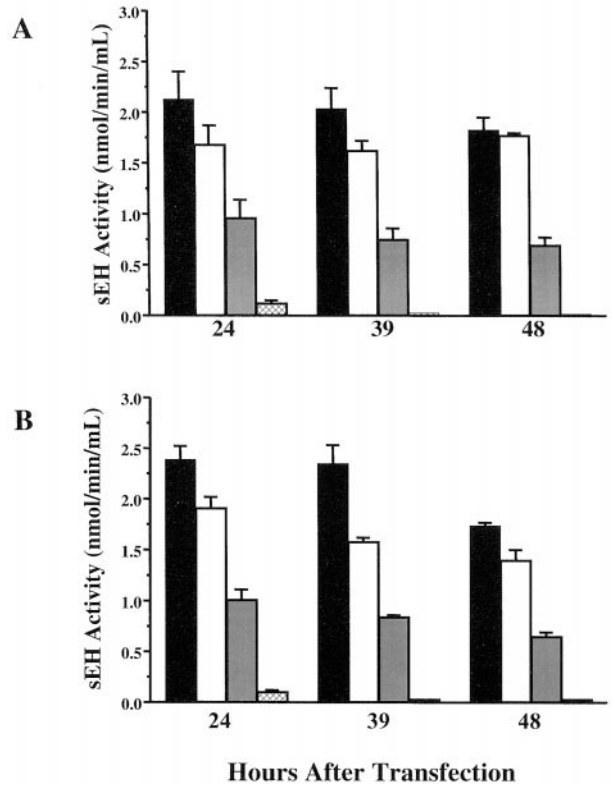

FIG. 1. **Transient expression of sEH proteins in CHO cells.** Wild-type (*black*), R287Q (*white*), and $Arg^{402-403ins}$ (*dark gray*) human sEH alleles were transiently transfected into CHO cells, as was the expression vector containing no insert (*hatched*). Cell suspensions, isolated at 24, 39, and 48 h following transfection, were assayed for sEH activity using *t*-SO as substrate. Cells concomitantly transfected with a CAT expression plasmid allowed normalization of transfection efficiency. Experiments were performed in duplicate Petri dishes (*A* and *B*), and *t*-SO measurements represent multiple assays/time point.

sEH Protein Stability over Time—To more fully characterize functional differences among the sEH alleles, and perhaps the mechanisms underlying activity differences, an analysis of isolated proteins over longer time was conducted. As before, transfection experiments using the 3 sEH alleles were performed with both CHO and COS-7 cells. Co-transfection with a CAT-expressing vector was used for normalization of expression. In these experiments, cells (2 plates/group) were harvested 40 h following transfection and stored at 4 °C on ice. At each analytical time point, an aliquot of cells from the different groups was assayed for sEH enzymatic activity (in triplicate).

Figs. 3 and 4 present the results obtained from extended time point analysis of transfected sEH alleles expressed in CHO and COS-7 cells, respectively. In both sets of experiments, all sEH proteins were catalytically active in the hydrolysis of *t*-SO, and the order of highest expression was identical to that observed previously: Wt > R287Q > $Arg^{402-403ins}$. The Wt and R287Q proteins possessed a similar pattern of sEH activity declination over time, although the activity profile for R287Q proteins demonstrated a greater rate of decay at later time points. The temporal profile observed for $Arg^{402-403ins}$ sEH proteins exhibited a more marked decline in enzymatic activity at earlier time points. In both cell types, but especially in

[2] S. Summerer and J. Meijer, personal communication.

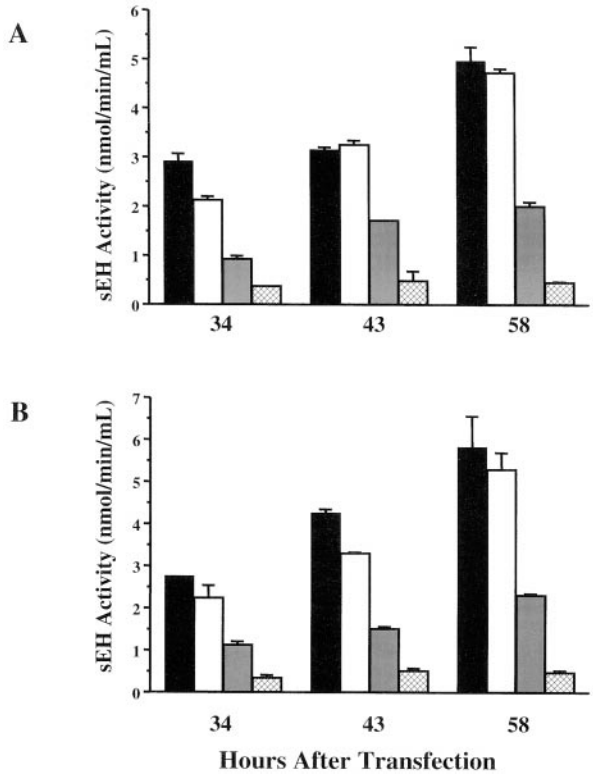

FIG. 2. **Transient expression of sEH proteins in COS-7 cells.** Expression plasmids containing the sEH alleles (wild-type, *black*; R287Q, *white*; $Arg^{402-403ins}$, *dark gray*; no insert, *hatched*) were transiently transfected into COS-7 cells and cell suspensions were isolated at 34, 43, and 58 h following transfection. *t*-SO activity was determined and normalized to CAT expression as described in the legend to Fig. 1.

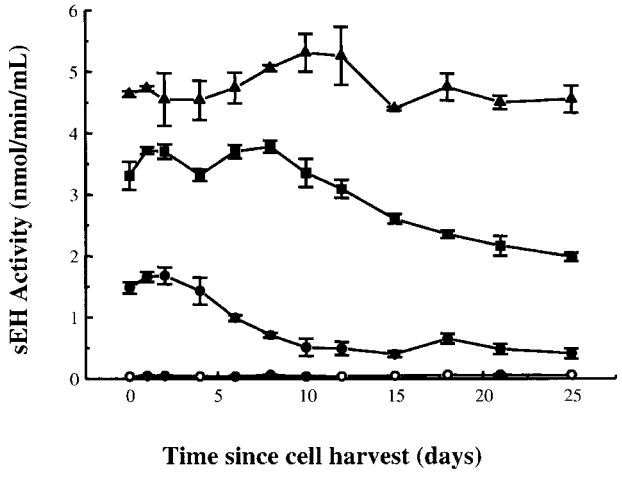

FIG. 3. **Stability of transiently expressed sEH proteins in CHO cells.** CHO cells were transfected with plasmids containing the Wt (*triangle*), R287Q (*square*), $Arg^{402-403ins}$ sEH (*circle*) alleles and vector only (*open circle*). Cell suspensions were isolated, placed at 4 °C, and assayed for *t*-SO-EH activity at various time points over 25 days. Normalization for transfection efficiency was performed by measurement of CAT activity from concomitantly transfected CAT-expressing plasmids.

COS-7 cells, $Arg^{402-403ins}$ sEH proteins exhibited a very diminished capacity to hydrolyze *t*-SO by 10 days post-cell harvest, and enzyme levels approached or reached background levels at subsequent time points.

Southern Blot Analysis—To assess the genetic complexity of *EPHX2* and evaluate the likelihood that there are related gene family members, restriction site polymorphism analysis was conducted in conjunction with Southern blotting. Genomic

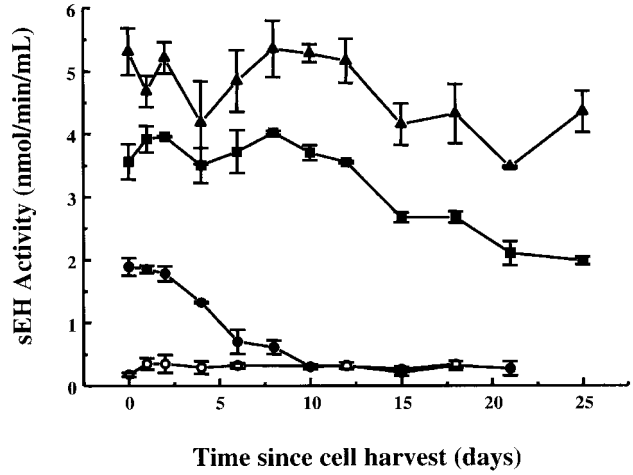

FIG. 4. **Stability of transiently expressed sEH proteins in COS-7 cells.** COS-7 cells were transfected with expression plasmids containing sEH alleles or no insert, according to the legend in Fig. 3. Cell suspensions were isolated, placed at 4 °C, and assayed for *t*-SO-EH activity at various time points over 25 days. Normalization to CAT expression was as described in the legend to Fig. 3.

DNA from 4 samples (127, 133, 135, and 137) was restricted with four enzymes (*Bam*HI, *Eco*RI, *Kpn*I, and *Sac*I). The banding patterns and fragment sizes observed following hybridization to radiolabeled sEH cDNA probe indicate that *EPHX2* is likely to be a single copy gene (Fig. 5). A potential *Sac*I polymorphism in the *EPHX2* gene was observed in 2 of the 4 DNA samples that were examined (samples 127 and 137 *versus* 133 and 135; see Fig. 5). Since *Sac*I restriction sites were not present in the sEH cDNAs analyzed in the current investigation, it is likely this polymorphism exists in nontranscribed portions of the *EPHX2* gene.

DISCUSSION

Generation and disposition of endogenous epoxide intermediates may represent an important regulatory component of diverse biological processes such as vascular reactivity (19), vascular inflammation (20), as well as leukotoxin-mediated alterations in vascular permeability and calcium homeostasis (37). The sEH enzyme likely functions to modulate endogenous epoxide levels derived from arachidonic and linoleic acids (21, 23, 38).

The human soluble epoxide hydrolase gene (*EPHX2*) spans >45 kilobases and contains 19 exons (25). In the current investigation, we report the presence of nucleotide variation in the *EPHX2* gene. Approximately 1.8 kilobases of sEH transcribed sequence was analyzed in 25 unrelated individuals (50 chromosomes) and eight variable loci were identified. Seven of these polymorphisms were localized to the protein coding region, and two resulted in amino acid changes. At position 287, a nonconservative glutamine residue was substituted in 8% of the alleles for the more commonly occurring arginine. A second nonconservative alteration, an in-frame trinucleotide insertion, results in a human sEH allelic protein containing an additional amino acid (arginine) following serine 402. Four percent of the sEH alleles examined contained this insertion. To our knowledge, insertion mutations of this nature are very rare in human proteins.

In addition to the data generated in the current study, two other human sEH sequences have been reported previously (3, 25). Alignment of these nucleotide sequences reveals discrepancies that are principally localized in 2 regions. Most differences occur in the 5′-nontranslated portion of the sEH transcript, and a second area of disagreement resides in a "GC"-rich segment of the protein-coding region. Sequence data for the

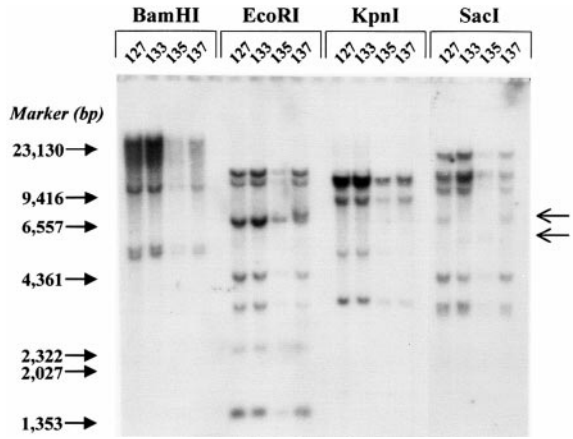

FIG. 5. **Genetic complexity of the *EPHX2* gene.** Human genomic DNA isolated from four samples (127, 133, 135, and 137) was individually restricted with four enzymes, size-separated by electrophoresis, and transferred to a membrane that was probed with a radiolabeled sEH specific cDNA. The banding patterns, and fragment sizes resulting from each restriction digest provide evidence that *EPHX2* is unlikely to be a gene family member. *Arrows* to the *right* of the figure indicate the position of faint bands, suggesting a common *Sac*I polymorphism exists in the *EPHX2* gene.

majority of sEH alleles determined in the present study are in agreement with that reported previously by Sandberg and Meijer (25), and therefore constitute what we refer to as the Wt sEH sequence. Three amino acid positions deduced from an sEH cDNA described earlier (3) were not observed in any alleles characterized in the current investigation (A5G, S257W, and Gly^{258del}). Possible explanations for these discrepancies include the existence of additional polymorphism(s) in human sEH proteins, and/or sequencing or cloning artifacts.

With respect to the amino acid polymorphisms identified in the current study, we demonstrate that the variation observed at each amino acid locus results in catalytically active sEH protein following transient transfection and expression of the recombinant proteins in either of two mammalian cell lines. However, *in vitro* expression of the Wt, R287Q, or $Arg^{402-403ins}$ sEH proteins resulted in distinct and reproducibly altered activity profiles when using *t*-SO as a model substrate. The Wt sEH protein exhibited consistently greater activity than either of the variant alleles. In particular, the $Arg^{402-403}$ sEH protein demonstrated markedly diminished activity relative to either the Wt or R287Q sEH enzymes. Increased protein lability, or reduction of catalytic efficiency is a logical explanation for these observations. To characterize the stability differences of the *in vitro* expressed sEH amino acid variants, cells were transfected with the individual sEH alleles and stored as cell suspensions at 4 °C. Cells expressing the variant alleles demonstrated reproducible differences in sEH enzymatic activity when assayed periodically over time. Although both variants were less stable compared with Wt protein in these experiments, the *t*-SO EH activity for the $Arg^{402-403ins}$ protein in particular declined more rapidly as compared with either the Wt or R287Q alleles, suggesting the $Arg^{402-403ins}$ sEH protein is inherently the least stable. In related experiments, we noted that the enzymatic activity of Wt or R287Q sEH proteins isolated from transfected cells was fairly resistant to freeze thawing procedures (approximately 80% activity maintained relative to fresh cells), whereas cells transfected with the $Arg^{402-403}$ allele only retained approximately 35% of initial activity (data not shown).

Alignment of mammalian sEH sequences reported for three species (4, 5, 25) reveals substantial conservation in deduced amino acid content (Fig. 6). Comparison of these mammalian sEH protein sequences offers potential insight to the importance of the newly identified human amino acid polymorphisms. Residue 287 in human sEH, the location of the Arg/Gln variation, resides within a highly conserved region of mammalian sEH proteins. Surrounding this polymorphic locus, an area encompassing more than 100 amino acids that is NH_2-terminal of the catalytic triad residues (39, 40), 96 amino acid positions are conserved, either absolutely or with semi-conservative substitution (Fig. 6). Similarly among these mammals, Arg^{403} is flanked by 31/32 conserved residues, although there is a prominent lack of sequence conservation to either side (see Fig. 6). Conserved sequence surrounding the polymorphic residues implies important function, structurally and/or catalytically, for these regions of mammalian sEH proteins.

Based on sequence alignments, it has been proposed that mammalian sEH is evolutionarily related to bacterial enzymes that belong to the α/β-hydrolase fold family of proteins (39, 41). Similar analyses suggest that the amino-terminal portion of mammalian sEH proteins is homologous to bacterial haloacid dehalogenase, while the carboxyl region is related to bacterial haloalkane dehalogenase (24). Presumably, a gene fusion event of the ancestral bacterial enzymes evolved to form present day mammalian sEH proteins (24). Recently, the protein crystal structure for mouse sEH has been solved (42), and results from this work support the notion that the mammalian sEH enzyme evolved as the fusion product of 2 discrete proteins. A "vestigial" NH_2-terminal region of the mouse sEH enzyme (with sequence homology to haloacid dehalogenase) is connected by a proline-rich linker to the catalytically active COOH-terminal domain (related to haloalkane dehalogenase) (42). The sequence alignments presented in Fig. 6 indicate that the NH_2-terminal region of mammalian sEH proteins is less conserved relative to the COOH-terminal region. The human sEH amino acid polymorphisms identified in the current investigation are both localized to the catalytically active COOH-terminal domain.

Because of the extensive sequence similarity among mammalian sEH proteins, the reported mouse sEH crystal structure (42) affords the opportunity to visualize the physical location of the human sEH polymorphisms and speculate as to possible functional consequences. The *top left panel* of Fig. 7 depicts the overall structure of mammalian sEH, which is a dimer in its native form (43). The two independent active sites in the dimer are indicated by the inhibitor (42), which is colored purple. The $Arg^{402-403ins}$ mutation ("RR", orange/red) lies within the "cap" region and is behind the active site, some 17 Å away, while the R287Q polymorphism ("R/Q") lies at the dimer interface, about 30 Å from each active site.

The *lower left panel* of Fig. 7 displays detail of the interface between the sEH monomers, and shows the observed hydrogen bond interactions for the Wt and predicted interactions for the mutated R287Q locus. The interface is generally hydrophobic, and burial of the polymorphic arginine or glutamine residue at the center of this interface (Fig. 7, *lower right*) signals the importance of the interaction. It is likely that the buried glutamic acid (Glu^{254}) has an unusual pK_a, and that the positively charged Arg^{287} is required to counter its expected negative charge. In addition to the charge differences following mutation from Arg to Gln, there are a number of specific hydrogen bonds that will change as well. The guanidinium side chain of Arg^{287} from one monomer extends into the interface and forms a hydrogen bond with the carbonyl oxygen of Gly^{256} of the other monomer. An sEH protein containing the Gln^{287} polymorphism, with the shorter side chain (relative to Arg^{287}), will not form this hydrogen bond across the dimer interface with Gly^{256}. Hydrogen bonding across the dimer interface from Arg^{287} in

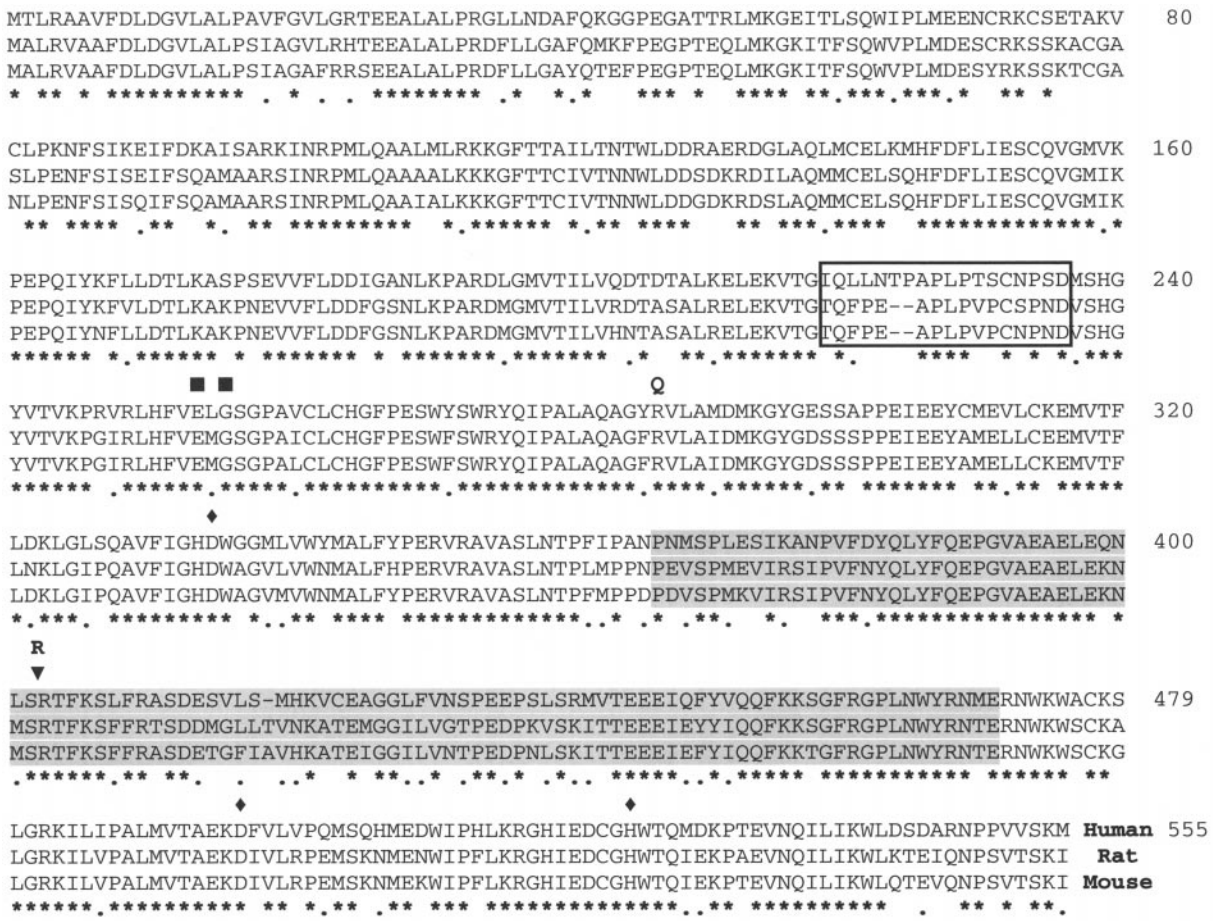

FIG. 6. **Sequence alignment of mammalian sEH proteins.** Human (25), rat (5), and mouse (4) sEH proteins are aligned showing residues that are conserved absolutely (*) or conservatively substituted (.), with gaps inserted as necessary to maximize alignment. The locations of the human polymorphisms are indicated by a "*Q*" or "*R*" *above* the top sequence. The *boxed* sequence identifies the proline-rich "hinge region" that separates the vestigial and catalytic domains, as described previously (42). A "cap" region, which forms a border of the "L"-shaped active site pocket described from the mouse crystal structure (42), contains the $Arg^{402-403}$ insertion and is shown in *gray* background. Amino acids comprising the catalytic triad (2) are designated by the *diamond symbols*. Glu^{254} and Gly^{256}, residues with potential bond interactions at the sEH dimer interface, are indicated by *solid boxes* above the human sequence.

the other monomer is repeated in the reverse orientation. Thus, the outer 2 hydrogen bonds shown in the *lower left panel* would not be possible in homodimeric proteins containing Gln^{287}.

Glu^{254} also forms a hydrogen bond interaction across the dimer interface with a corresponding Glu^{254} from the other monomer. A second hydrogen bond interaction by Glu^{254} is predicted to occur with residue 287, within a single monomer. In this instance, either Arg^{287} or Gln^{287} can successfully participate in the respective bond.

A number of findings suggest that arginine residues at protein interfaces may be particularly important. The exact details will be peculiar to an individual protein but, in general, arginine replacement at an interface can be destabilizing, and may even effect long range alterations. For example, in thymidylate synthase, mutations of two different interfacial arginine residues lowers the stability toward unfolding (44). A compilation of alanine-scanning mutagenesis of residues at protein interfaces, has shown that not only are there "hot-spots" at the center of an interaction surface (surrounded by a water-excluding "O-ring" of residues), but the most likely residues found at the center are Tyr, Trp, and Arg (45). Residues in hot spots contribute more to the binding energy than residues outside this region. According to this analysis (45), glutamine is an under-represented residue in dimer interfaces and one would conclude that it may be particularly destabilizing. The sEH R287Q is in fact quite far from the active site. Comparison of gently energy minimized structures of the mutated and unmutated forms show small perturbations of the active site residues that could cause diminished activity, but in the absence of an actual structure from the R287Q protein these calculations are only suggestive. The possibility of long range effects, however, is supported by an analysis of disease-causing mutations at the dimer interface of glucose-6-phosphate dehydrogenase that decrease stability. Site-directed mutations that effected an increase in stability (for example, by complementing a charge) were shown to decrease the ability of NADP (some 20 Å from the dimer interface) to stabilize the dimer (46).

The *upper right panel* of Fig. 7 shows the detail of molecular interactions in the vicinity of Arg^{403} of a single sEH monomer. The wild type Arg^{403} structure is shown in *green*, while predicted changes resulting from the mutation $Arg^{402-403ins}$ are superimposed and colored *red*. The $Arg^{402-403ins}$ creates a bulge in the polypeptide chain forcing the side chain of the second Arg residue to point outward, the adjacent helices to reorient, and other residues to re-pack including those in the active site region. Each of the residues comprising the catalytic triad, as well as Tyr^{466} (which may participate in the activation of the epoxide substrate), is displaced relative to those in Wt sEH proteins containing only the single Arg^{403}. Misalignment of these catalytic residues would logically be expected to alter the efficiency by which hydrolysis occurs. Moreover, if the shifted residues also produced misalignment of the cap, which forms one side of the substrate/inhibitor binding pocket, an additional cause of lowered activity is possible.

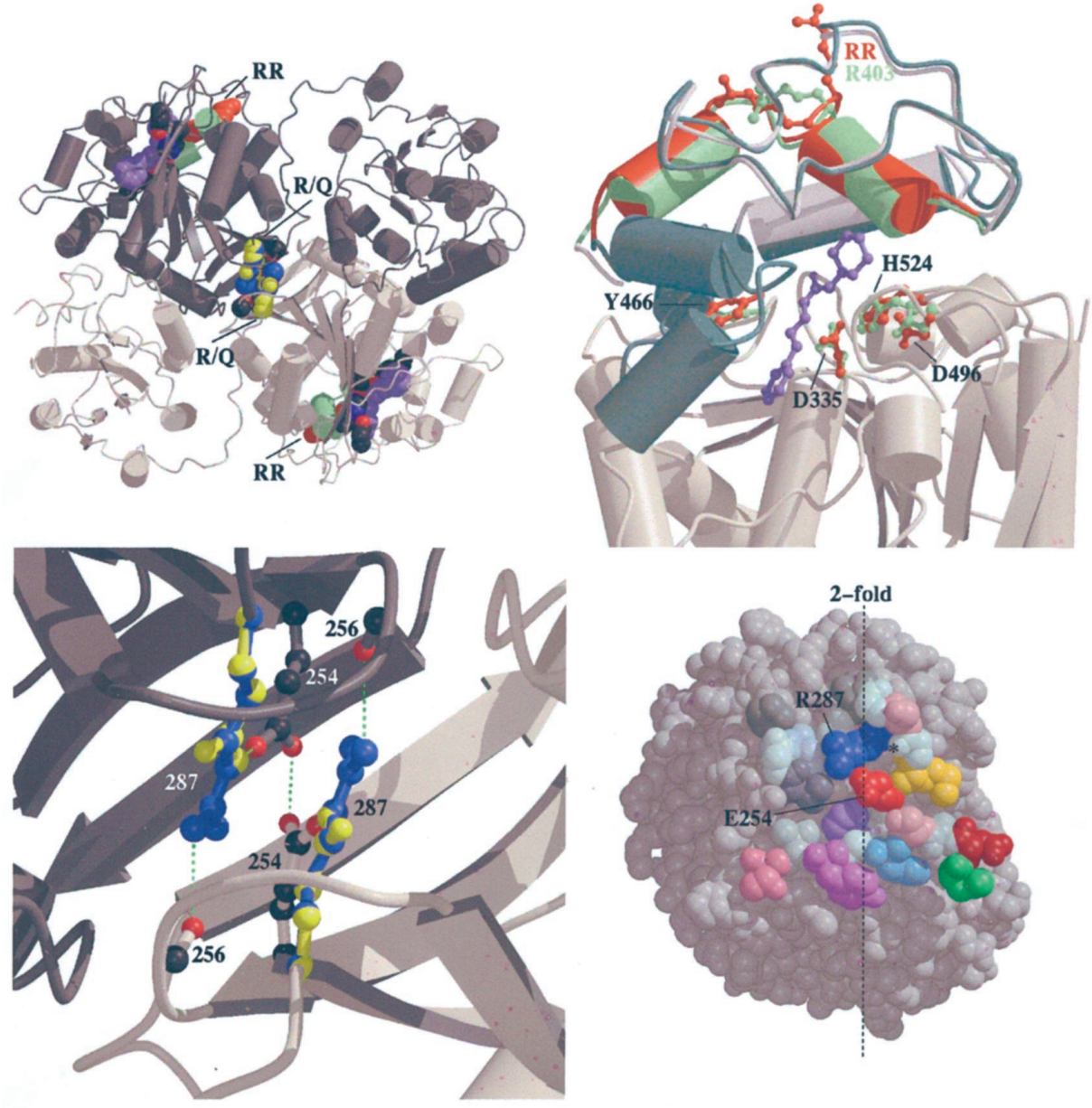

FIG. 7. **Three-dimensional location of sEH amino acid polymorphisms and predicted effects.** By analogy to the crystal structure previously reported (PDB code 1CR6) (49) for mouse sEH (42), the location of the human sEH amino acid polymorphisms are shown. *Top left panel,* the sEH dimer is depicted with one monomer colored in *dark gray* and the other in *light gray*. The active site region for each monomer is indicated by the *purple*-colored inhibitor, *N*-cyclohexyl-*N′*-(3-phenyl)propylurea) (42). The polymorphic loci Arg^{403} (*green*), $Arg^{402-403ins}$ (*red*), Arg^{287} (*blue*), and Gln^{287} (*yellow*) are shown. *Lower left panel,* the interface between two sEH monomers, looking down along the 2-fold relating the monomers, in the immediate vicinity of the 287 locus polymorphism, is shown in detail. The side chain of Arg^{287} (*blue*) forms hydrogen bond interactions across the interface with Gly^{256} of its partnered monomer. The side chain of Gln^{287} (*yellow*) is too short to interact with Gly^{256}. A hydrogen bond interaction from either sEH 287 residue (Arg or Gln) to Glu^{254} of the same monomer is predicted to be undisturbed by the polymorphism. *Lower right panel,* view of the monomer surface, at the dimer interface. Residues that contact the apposing monomer are colored (*pink*, Ser/Thr; *yellow*, Met; *purple*, Tyr/Phe; *light gray*/*white,* Ala/Pro/Ile/Leu/Gly) and those not in contact are *dark gray*. Arg^{287} is *blue*, Glu^{254} is *red*, and the *asterisk* marks the carbonyl oxygen to which Arg^{287} from the other monomer is bound. The *vertical dashed line* denotes the 2-fold axis that relates the two monomers. *Upper right panel,* the effect of inserting an additional Arg residue following Ser^{402} in the human sEH protein is detailed. The "cap" region, into which the insertion is made, is shown in *blue-green*. Structures associated with the wild-type protein (Arg^{403}) are shown in *green*, while the postulated location of $Arg^{402-403ins}$ protein is depicted in *red*. The anticipated effects of the Arg insertion include a reorientation of the two helices on either side of the polymorphic locus, altering the position of nearby amino acids, and ultimately misaligning active site residues (*red* or *green* according to the polymorphic allele). To evaluate the effects of the Arg insertion on active site residues, or of the Arg/Gln mutation, the Wt and "mutated" structures were gently energy minimized using the software Molecular Operating Environment (available from the Chemical Computing Group, Montreal, Canada) keeping the non-catalytic domains fixed as well as all sulfur atoms in the structure. Mutations in the mouse sEH crystal structure (42) were made using the program "O" (50). Drawings were made using MOLSCRIPT (51) and Raster3D (52).

Evidence for polymorphism in human sEH protein reported herein, and that sEH is a dimeric protein *in vivo* (43), establishes that there are multiple possibilities for dimer composition in heterozygous individuals. An individual who is heterozygous Arg/Gln at the 287 locus would be expected to have sEH dimerized proteins that have any of three combinations: Arg/Arg, Arg/Gln, and Gln/Gln. Clearly, individuals homozygous for the Gln^{287} polymorphism would possess monomers with only that residue at the dimer interface which we predict would result in a less stable configuration.

Genetic polymorphisms in human biotransformation enzymes, including cytochrome P450s and glutathione trans-

ferases, are becoming increasingly well characterized as to their functional impacts and potential inter-relationships (47, 48). We previously identified 2 amino acid polymorphisms in the human mEH protein (33). The human sEH amino acid variants identified in the current study should facilitate comparative analyses of epoxide disposition mediated by these important polymorphic hydrolases. With consideration to the anticipated prominent role of sEH in regulating the disposition of biologically active epoxides, further investigations are required to fully characterize the impact of the identified genetic polymorphisms on substrate-dependent functional activity, protein dimerization, and potential relationships to inflammatory and vascular disease processes that may involve alterations of normal epoxide metabolism in mammalian cells.

REFERENCES

1. Parkinson, A. (1996) in *Biotransformation of Xenobiotics: Casarett & Doull's Toxicology* (Klaassen, C. D., ed) pp. 113–186, McGraw-Hill, Inc., New York
2. Hammock, B. D., Storms, D. H., and Grant, D. F. (1997) in *Comprehensive Toxicology* (Sipes, I. G., McQueen, C. A., and Gandolfi, A. J., eds) Vol. 3, pp. 283–305, Elsevier Sciences, Inc., New York
3. Beetham, J. K., Tian, T., and Hammock, B. D. (1993) *Arch. Biochem. Biophys.* **305,** 197–201
4. Grant, D. F., Storms, D. H., and Hammock, B. D. (1993) *J. Biol. Chem.* **268,** 17628–17633
5. Knehr, M., Thomas, H., Arand, M., Gebel, T., Zeller, H. D., and Oesch, F. (1993) *J. Biol. Chem.* **268,** 17623–17627
6. Misawa, E., Chan Kwo Chion, C. K., Archer, I. V., Woodland, M. P., Zhou, N. Y., Carter, S. F., Widdowson, D. A., and Leak, D. J. (1998) *Eur. J. Biochem.* **253,** 173–183
7. Rink, R., Fennema, M., Smids, M., Dehmel, U., and Janssen, D. B. (1997) *J. Biol. Chem.* **272,** 14650–14657
8. Stapleton, A., Beetham, J. K., Pinot, F., Garbarino, J. E., Rockhold, D. R., Friedman, M., Hammock, B. D., and Belknap, W. R. (1994) *Plant J.* **6,** 251–258
9. Kiyosue, T., Beetham, J. K., Pinot, F., Hammock, B. D., Yamaguchi-Shinozaki, K., and Shinozaki, K. (1994) *Plant J.* **6,** 259–269
10. Larsson, C., White, I., Johansson, C., Stark, A., and Meijer, J. (1995) *Hum. Genet.* **95,** 356–358
11. Hartsfield, J. K., Jr., Sutcliffe, M. J., Everett, E. T., Hassett, C., Omiecinski, C. J., and Saari, J. A. (1998) *Cytogenet. Cell Genet.* **83,** 44–45
12. Watabe, T., Kanai, M., Isobe, M., and Ozawa, N. (1981) *J. Biol. Chem.* **256,** 2900–2907
13. Pace-Asciak, C. R., and Lee, W. S. (1989) *J. Biol. Chem.* **264,** 9310–9313
14. Mueller, M. J., Andberg, M., and Haeggstrom, J. Z. (1998) *J. Biol. Chem.* **273,** 11570–11575
15. Capdevila, J. H., Falck, J. R., and Estabrook, R. W. (1992) *FASEB J.* **6,** 731–736
16. Fitzpatrick, F. A., and Murphy, R. C. (1988) *Pharmacol. Rev.* **40,** 229–241
17. McGiff, J. C. (1991) *Annu. Rev. Pharmacol. Toxicol.* **31,** 339–369
18. VanRollins, M., Kaduce, T. L., Fang, X., Knapp, H. R., and Spector, A. A. (1996) *J. Biol. Chem.* **271,** 14001–14009
19. Fisslthaler, B., Popp, R., Kiss, L., Potente, M., Harder, D. R., Fleming, I., and Busse, R. (1999) *Nature* **401,** 493–497
20. Node, K., Huo, Y., Ruan, X., Yang, B., Spiecker, M., Ley, K., Zeldin, D. C., and Liao, J. K. (1999) *Science* **285,** 1276–1279
21. Weintraub, N. L., Fang, X., Kaduce, T. L., VanRollins, M., Chatterjee, P., and Spector, A. A. (1999) *Am. J. Physiol.* **277,** H2098–H2108
22. Kosaka, K., Suzuki, K., Hayakawa, M., Sugiyama, S., and Ozawa, T. (1994) *Mol. Cell Biochem.* **139,** 141–148
23. Moghaddam, M. F., Grant, D. F., Cheek, J. M., Greene, J. F., Williamson, K. C., and Hammock, B. D. (1997) *Nat. Med.* **3,** 562–566
24. Beetham, J. K., Grant, D., Arand, M., Garbarino, J., Kiyosue, T., Pinot, F., Oesch, F., Belknap, W. R., Shinozaki, K., and Hammock, B. D. (1995) *DNA Cell Biol.* **14,** 61–71
25. Sandberg, M., and Meijer, J. (1996) *Biochem. Biophys. Res. Commun.* **221,** 333–339
26. Mertes, I., Fleischmann, R., Glatt, H. R., and Oesch, F. (1985) *Carcinogenesis* **6,** 219–223
27. Norris, K. K., DeAngelo, T. M., and Vesell, E. S. (1989) *J. Clin. Invest.* **84,** 1749–1756
28. Kramer, A., Frank, H., Setiabudi, F., Oesch, F., and Glatt, H. (1991) *Biochem. Pharmacol.* **42,** 2147–2152
29. Fahlstadius, P. (1988) *Lipids* **23,** 1015–1018
30. Wrensch, M. R., Petrakis, N. L., Gruenke, L. D., Miike, R., Ernster, V. L., King, E. B., Hauck, W. W., Craig, J. C., and Goodson, W. H., III (1989) *Cancer Res.* **49,** 2168–2174
31. Hassett, C., Lin, J., Carty, C. L., Laurenzana, E. M., and Omiecinski, C. J. (1997) *Arch. Biochem. Biophys.* **337,** 275–283
32. Hassett, C., Richter, R. J., Humbert, R., Chapline, C., Crabb, J. W., Omiecinski, C. J., and Furlong, C. E. (1991) *Biochemistry* **30,** 10141–10149
33. Hassett, C., Aicher, L., Sidhu, J. S., and Omiecinski, C. J. (1994) *Hum. Mol. Genet.* **3,** 421–428
34. Gill, S. S., Ota, K., and Hammock, B. D. (1983) *Anal. Biochem.* **131,** 273–282
35. Antonarakis, S. E. (1998) *Hum. Mutat.* **11,** 1–3
36. Holland, P. M., Abramson, R. D., Watson, R., and Gelfand, D. H. (1991) *Proc. Natl. Acad. Sci. U. S. A.* **88,** 7276–7280
37. Morisseau, C., Goodrow, M. H., Dowdy, D., Zheng, J., Greene, J. F., Sanborn, J. R., and Hammock, B. D. (1999) *Proc. Natl. Acad. Sci. U. S. A.* **96,** 8849–8854
38. Zeldin, D. C., Wei, S., Falck, J. R., Hammock, B. D., Snapper, J. R., and Capdevila, J. H. (1995) *Arch. Biochem. Biophys.* **316,** 443–451
39. Lacourciere, G. M., and Armstrong, R. N. (1994) *Chem. Res. Toxicol.* **7,** 121–124
40. Pinot, F., Grant, D. F., Beetham, J. K., Parker, A. G., Borhan, B., Landt, S., Jones, A. D., and Hammock, B. D. (1995) *J. Biol. Chem.* **270,** 7968–7974
41. Arand, M., Grant, D. F., Beetham, J. K., Friedberg, T., Oesch, F., and Hammock, B. D. (1994) *FEBS Lett.* **338,** 251–256
42. Argiriadi, M. A., Morisseau, C., Hammock, B. D., and Christianson, D. W. (1999) *Proc. Natl. Acad. Sci. U. S. A.* **96,** 10637–10642
43. Meijer, J., and DePierre, J. W. (1985) *Eur. J. Biochem.* **148,** 421–430
44. Prasanna, V., Gopal, B., Murthy, M. R., Santi, D. V., and Balaram, P. (1999) *Proteins* **34,** 356–368
45. Bogan, A. A., and Thorn, K. S. (1998) *J. Mol. Biol.* **280,** 1–9
46. Scopes, D. A., Bautista, J. M., Naylor, C. E., Adams, M. J., and Mason, P. J. (1998) *Eur. J. Biochem.* **251,** 382–388
47. Daly, A. K., Cholerton, S., Gregory, W., and Idle, J. R. (1993) *Pharmacol. Ther.* **57,** 129–160
48. Gonzalez, F. J. (1997) *Reprod. Toxicol.* **11,** 397–412
49. Berman, H. M., Westbrook, J., Feng, Z., Gilliland, G., Bhat, T. N., Weissig, H., Shindyalov, I. N., and Bourne, P. E. (2000) *Nucleic Acids Res.* **28,** 235–242
50. Jones, T. A., Zou, J. Y., Cowan, S. W., and Kjeldgaard, M. (1991) *Acta Crystallogr* **A47,** 110–119
51. Kraulis, P. (1991) *J. Appl. Cryst.* **24,** 946–950
52. Merritt, E. A., and Murphy, M. E. P. (1994) *Acta Crystallogr. Sect. D* **50,** 869–873